Conductivity noise across temperature-driven transitions of rare-earth nickelate heterostructures

Gopi Nath Daptary,[1] Siddharth Kumar,[1] M. Kareev,[2] J. Chakhalian,[2] Aveek Bid,[1,*] and S. Middey[1,†]
[1]*Department of Physics, Indian Institute of Science, Bengaluru 560012, India*
[2]*Department of Physics and Astronomy, Rutgers University, Piscataway, New Jersey 08854, USA*

(Received 18 March 2019; revised manuscript received 19 June 2019; published 3 September 2019)

The metal-insulator transition (MIT) of bulk rare-earth nickelates is accompanied by a simultaneous charge ordering (CO) transition. We have investigated low-frequency resistance fluctuations (noise) across the MIT and magnetic transition of [$EuNiO_3/LaNiO_3$] superlattices, where selective suppression of charge ordering has been achieved by mismatching the superlattice periodicity with the periodicity of charge ordering. We have observed that irrespective of the presence or absence of long-range CO, the noise magnitude is enhanced by several orders with a strong non-$1/f$ (f = frequency) component when the system undergoes a MIT and magnetic transition. The higher-order statistics of resistance fluctuations reveal the presence of strong non-Gaussian components in both cases, further indicating inhomogeneous electrical transport arising from the electronic phase separation. Specifically, we find almost three orders of magnitude smaller noise in the insulating phase of the sample without long-range CO compared to the sample with CO. These findings suggest that digital synthesis can be a potential route to implement electronic transitions of complex oxides for device application.

DOI: 10.1103/PhysRevB.100.125105

I. INTRODUCTION

The metal-insulator transition (MIT), observed in complex materials as a function of temperature, chemical doping, electrostatic gating, magnetic field, light, pressure, epitaxy, etc., has remained a topic of paramount interest for decades [1,2]. The complexity of the mechanism of the MIT in the rare-earth nickelate series has attracted significant attention in recent years [3,4]. In the bulk form, $RNiO_3$, with R = Sm, Eu, Lu, Y, etc., undergoes a first-order transition from an orthorhombic, metallic phase without charge ordering to a monoclinic, insulating phase with a rocksalt-type charge ordering (CO) [5,6]. A magnetic transition (paramagnetic to E' antiferromagnetic) occurs at a lower temperature. Moreover, four transitions appear simultaneously in bulk $NdNiO_3$ and $PrNiO_3$. In order to explain the origin of this peculiar MIT, the importance of the structural transition [7], electron correlations [8], charge ordering [9,10], distribution of ligand holes [11–16], polaron condensation [17], Fermi surface nesting [18–20], etc., has been emphasized by different types of experimental probes and theoretical methods. Interestingly, it was demonstrated recently that a MIT without any long-range CO and structural symmetry change can be obtained in the artificial structure of $RNiO_3$ by mismatching the periodicity of the heterostructure and the periodicity of rocksalt-type CO [21]. Apart from the interest arising from the aspect of fundamental physics, $RNiO_3$-based heterostructures also show excellent potential for electronic applications [3,4,22–25].

The low-frequency $1/f$ noise not only is used for semiconductor device characterizations [26] but also acts as a powerful tool to probe exotic phenomena like electronic phase separation [27], structural phase transition [28], charge density wave [29], superconductor-normal-state phase transition [30,31], etc. The frequency dependence of the power spectral density (PSD) $S_R(f)$ (described later) arises due to finite relaxation of the fluctuating variable. According to the central limit theorem, the fluctuation statistics of a system is Gaussian if the fluctuators are independent of each other [32]. However, the presence of any correlations due to magnetic, electronic, or structural interactions in the system would result in non-Gaussian statistics of time-dependent fluctuations. This information can be extracted from higher-order statistics of resistance fluctuations via the "second spectrum" [33,34]. The phase transitions of $SmNiO_3$ and $NdNiO_3$ single-crystalline films were studied by such noise and second-spectrum measurements [35–37]. The extremely large magnitude of the noise and the second spectrum were attributed to the coexistence of metal and insulator phases near the electronic transition temperature. Such a $1/f$ noise study can also provide crucial information about the length scale of charge ordering, as reported previously for colossal magnetoresistive (CMR) manganites [38].

In this work, we report on resistance fluctuations across the electronic and magnetic transitions of 2 uc $EuNiO_3$/1 uc $LaNiO_3$ (2ENO/1LNO) and 1 uc $EuNiO_3$/1 uc $LaNiO_3$ (1ENO/1LNO) films (where uc = unit cell in pseudocubic notation). The 1ENO/1LNO superlattice (SL) exhibits four simultaneous transitions [21], similar to bulk $NdNiO_3$ and $PrNiO_3$. On the other hand, the 2ENO/1LNO SL is a rare example, which undergoes a first-order MIT without any long-range CO and remains monoclinic in both the metallic

*aveek@iisc.ac.in
†smiddey@iisc.ac.in

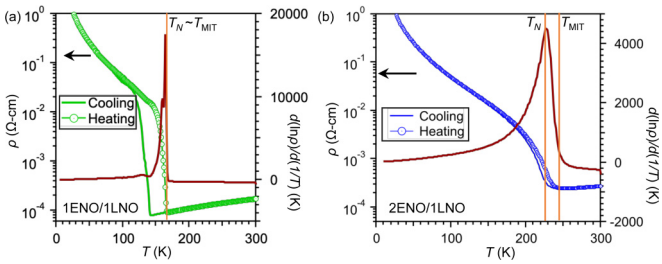

FIG. 1. Resistivity ρ as a function of temperature for (a) 1ENO/1LNO and (b) 2ENO/1LNO. The corresponding $d\ln(\rho)/d(1/T)$ is also plotted as a function of T [right axis of (a) and (b)].

and insulating phases [21]. We have observed the random telegraphic noise (RTN) as well as the non-Gaussian component (NGC) of noise near the MIT of these films, which confirms the coexistence of spatially separated metallic and insulating phases in both samples. Importantly, we have found that the energy barrier separating these electronic phases and the associated length scale of nanoscopic phase separation are similar in both samples. However, the noise magnitude in the insulating phase of 2ENO/1LNO SL is *three orders of magnitude smaller* than the corresponding noise in 1ENO/1LNO SL, suggesting that the system with a MIT without long-range charge ordering would be a better candidate for practical device applications. Interestingly, the higher-order statistics of resistance fluctuations (quantified as the second spectrum) becomes maximum near the antiferromagnetic transition temperature T_N of 2ENO/1LNO SL, implying a certain role of E' magnetic ordering in opening the gap in the multiband Fermi surface.

II. EXPERIMENTAL DETAILS

The [2 uc $EuNiO_3$/1 uc $LaNiO_3$] x12 (2ENO/1LNO) and [1 uc $EuNiO_3$/1 uc $LaNiO_3$]x18 (1ENO/1LNO) SLs were grown on a single-crystalline $NdGaO_3$ (110) substrate by pulsed laser interval deposition. The details of the growth conditions and characterizations can be found in Refs. [21,39,40]. The resistance and noise measurements were performed in a cryofree 4 K system.

III. RESULTS AND DISCUSSION

Figures 1(a) and 1(b) show the temperature-dependent resistivity ρ for 1ENO/1LNO and 2ENO/1LNO films, respectively. From now on, we discuss the results of the heating run. As can be seen, 1ENO/1LNO and 2ENO/1LNO SLs undergo first-order insulator to metal transitions around 165 and 245 K, respectively. The magnetic transition temperatures T_N are found to be 165 K for 1ENO/1LNO and 225 K for the 2ENO/1LNO SL from the $d\ln(\rho)/d(1/T)$ vs T plot [39,41,42] [see the right axes of Figs. 1(a) and 1(b)].

To probe the nature of the electrical transport, we measured low-frequency resistance fluctuations of 1ENO/1LNO and 2ENO/1LNO films using the standard four-probe lock-in amplifier (LIA) technique [34]. This technique allows us to measure both the sample and background noise. The sample was current biased (I) with an excitation frequency $f^* \sim$ 220 Hz. The voltage fluctuations $\delta V(t)$ arise at the sideband of f^* after the signal is demodulated from the LIA. The output of the LIA was digitized to a high-speed analog to digital converter (ADC) and stored to get the time series of voltage fluctuations $\delta V(t)$. The time series of voltage fluctuations $\delta V(t)$ was converted to the time series of resistance fluctuations $\delta R(t)$ as $\delta R(t) = \delta V(t)/I$. In Fig. 2(a), we plot the

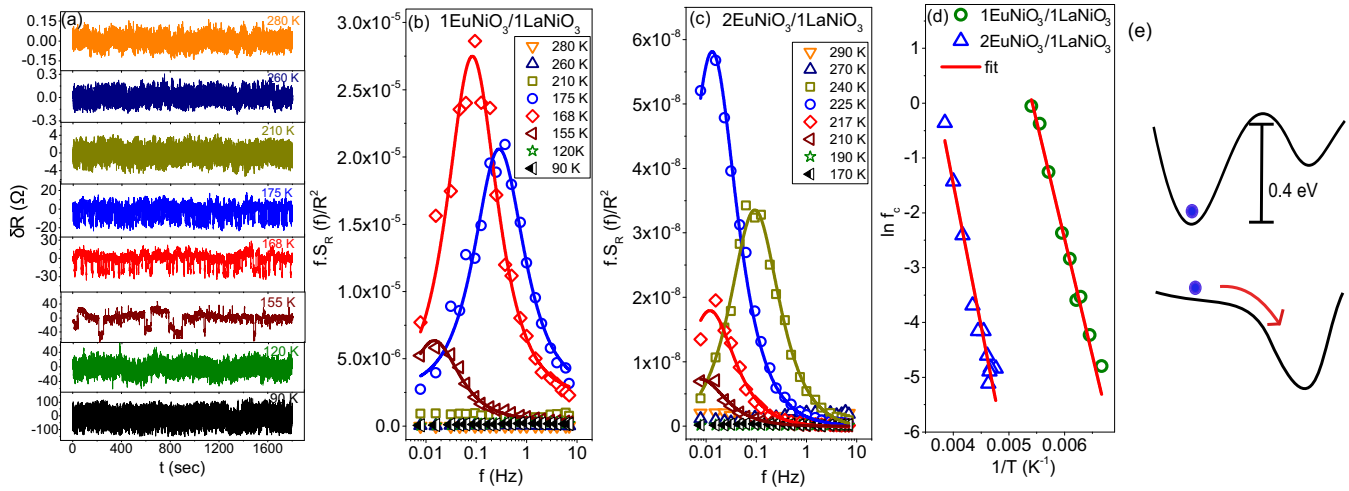

FIG. 2. (a) Time series of resistance fluctuations at a few representative values of T of $1EuNiO_3/1LaNiO_3$. (b) and (c) Scaled PSD of resistance fluctuations $fS_R(f)/R^2$ as a function of frequency at a few representative values of T for $1EuNiO_3/1LaNiO_3$ and $2EuNiO_3/1LaNiO_3$ respectively. The solid lines are the fits to the data with Eq. (1). For details, see text. (d) Plot of f_c as a function of the inverse temperature on a semilog scale. Solid lines are an Arrhenius fit to the data as discussed in the text. (e) A schematic energy diagram of two level states: insulating and metallic states. Top and bottom diagrams represent the position of the electron (solid circle) while the system is in insulating and metallic states, respectively.

time series of resistance fluctuations at different temperatures for the 1ENO/1LNO SL. As can clearly be seen, each time series for $T > T_{\mathrm{MIT}}$ consists of random resistance fluctuations about the average value. Similar features are also seen in the case of the 2ENO/1LNO SL for $T > T_{\mathrm{MIT}}$ (see the Appendix, Fig. 5). Interestingly, we observe the appearance of RTN with the resistance fluctuations between two states in the temperature range 140 K $< T <$ 200 K for the 1ENO/1LNO SL and 200 K $< T <$ 260 K for the 2ENO/1LNO SL. These RTNs are absent below 140 K for the 1ENO/1LNO SL and 195 K for the 2ENO/1LNO SL. Such a RTN was also reported for other systems, e.g., manganites [38], and two-dimensional superconductors [29], where the system can fluctuate between two distinct phases. Surprisingly, the ratio of the temperature (T_{RTN}) where RTN starts to appear and T_{MIT} is very similar (∼0.85) for both 1ENO/1LNO and 2ENO/1LNO SLs.

To understand the origin of the RTN, we investigated the PSD of the resistance fluctuations $S_R(f)$. At each T, the resistance fluctuations were recorded for 30 min. The data were decimated and digitally filtered to eliminate the 50 Hz line frequency. $S_R(f)$ was calculated using the fast Fourier transformation technique from the filtered time series [34]. The minimum and maximum frequencies of the noise measurement are 4 mHz and 8 Hz, respectively. In order to accentuate any deviation from the $1/f$ nature of the spectrum, we plot the quantity $fS_R(f)/R^2$ as a function of f at a few representative temperatures for 1ENO/1LNO [Fig. 2(b)] and 2ENO/1LNO [Fig. 2(c)]. For $T \gg T_{\mathrm{MIT}}$, the PSD $S_R(f)$ follows $1/f^{\alpha}$ dependence, with $\alpha \sim 1$ for both samples. However, a strong deviation from the $1/f$ dependence of the spectral power has been found within the temperature range 140 K $< T <$ 200 K for the 1ENO/1LNO SL and 200 K $< T <$ 260 K for the 2ENO/1LNO SL. Interestingly, these are the same temperature ranges where the RTN is also observed. Further analysis shows that $S_R(f)$ in this temperature range has two components: (a) the $1/f$ component and (b) a Lorentzian term with a corner frequency f_c,

$$\frac{S_R(f)}{R^2} = \frac{A}{f} + \frac{Bf_c}{f^2 + f_c^2}. \tag{1}$$

The constants A and B are the measure of the relative strength of the two terms. The second term arises from a single-frequency fluctuator with frequency f_c. f_c can be extracted by the fitting (solid line) of the experimental data (symbols) using Eq. (1), as shown in Figs. 2(b) and 2(c) for 1ENO/1LNO and 2ENO/1LNO films, respectively, for several temperatures.

The linear relation between $\ln(f_c)$ and $1/T$ [Fig. 2(d)] demonstrates the thermally activated behavior of f_c ($f_c = f_0 e^{-E_a/k_B T}$, where k_B is Boltzmann's constant) with an activation energy $E_a \sim 0.42 \pm 0.03$ eV for both samples. A similar value of E_a was also observed in CMR manganite when it underwent charge order transition [38]. The physical significance of this activated behavior can be visualized as follows. For $T \ll T_{\mathrm{MIT}}$, the entire volume is spatially insulating, and the resistance fluctuations are completely random. When the temperature reaches T_{RTN}, metallic clusters start to nucleate in the insulating background. Such a metastable metallic phase is separated from the insulating phase by the energy barrier

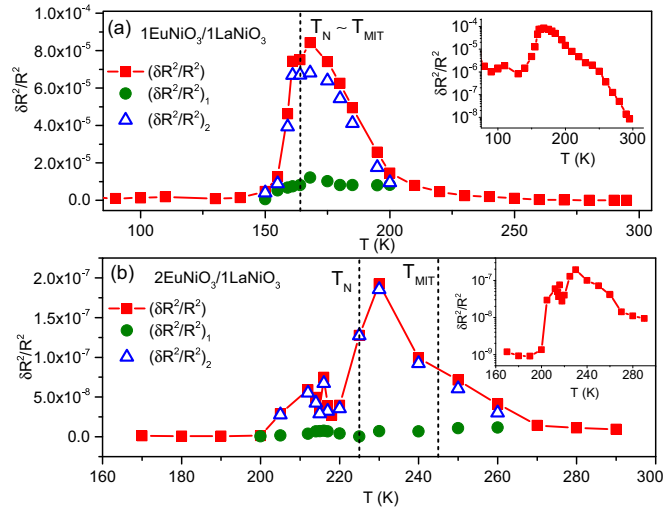

FIG. 3. (a) and (b) Temperature dependence of the total noise ($\frac{\delta R^2}{R^2}$) (red solid squares), $1/f$ noise component ($\frac{\delta R^2}{R^2}$)$_1$ (green solid circles), and Lorentzian component ($\frac{\delta R^2}{R^2}$)$_2$ (blue open triangles) of 1EuNiO$_3$/1LaNiO$_3$ and 2EuNiO$_3$/1LaNiO$_3$, respectively. For details see the text. Insets in (a) and (b) show the semilog plot of the total noise as a function of temperature.

E_a [top diagram in Fig. 2(e)], and the competition between these two phases results in RTN in the resistance fluctuations. For $T \gg T_{\mathrm{MIT}}$, the system is again completely in the metallic state [Fig. 2(e), bottom], and fluctuations become random again. In the subsequent paragraphs, we discuss the results of the integrated PSD and second spectrum to strengthen this picture. Details of the quantitative estimation of the noise level can be found in the Appendix.

The PSD of resistance fluctuations was further integrated over the measurement bandwidth to obtain the relative variance $\frac{\delta R^2}{R^2}$ (noise) $= \frac{1}{R^2}\int S_R(f)df$. As can be seen from the insets of Figs. 3(a) and 3(b), the magnitude of noise in the insulating phase of the 1ENO/1LNO SL is 10^3 times larger than the observed noise in the insulating phase of the 2ENO/1LNO SL. The noise value remains almost constant up to $T \sim 0.85T_{\mathrm{MIT}}$ for both samples. While the noise is maximized around $T_{\mathrm{MIT}} \sim 165$ K for the 1ENO/1LNO SL, the peak for the 2ENO/1LNO SL appears around 230 K, which is 15 K lower than $T_{\mathrm{MIT}} \sim 245$ K. Interestingly, this 2ENO/1LNO sample also shows an additional noise peak around 210 K, which is again 15 K lower than $T_N \sim 225$ K. At this moment, the reason for this shift between the transition temperature obtained from the resistivity measurement and the temperature of the noise peak remains unclear. It may be related to the resistance fluctuations due to short-range charge orderings [43] in the insulating phase of this sample. In spite of the strong difference in the noise magnitude in insulating phases of 1ENO/1LNO and 2ENO/1LNO films, noise at 300 K has a similar order of magnitude (∼10^{-8}) in both samples. In the temperature range $0.85 \lesssim T/T_{\mathrm{MIT}} \lesssim 1.1$, the total noise $\frac{\delta R^2}{R^2}$ behaves as $\frac{\delta R^2}{R^2} = \int_{f_{\min}}^{f_{\max}} \frac{A}{f}df + \int_{f_{\min}}^{f_{\max}} \frac{Bf_c}{f^2+f_c^2}df = (\frac{\delta R^2}{R^2})_1 + (\frac{\delta R^2}{R^2})_2$ for both samples. The temperature dependence of the total noise $\frac{\delta R^2}{R^2}$, the contribution of the $1/f$

component $(\frac{\delta R^2}{R^2})_1$, and the Lorentzian component $(\frac{\delta R^2}{R^2})_2$ are shown in Figs. 3(a) and 3(b). It is remarkable that noise in the temperature range $0.85 \lesssim T/T_{\mathrm{MIT}} \lesssim 1.1$ predominantly arises from the Lorentzian component with a negligible contribution from the $1/f$ term.

We note that the noise close to T_{MIT} is two to four orders larger than that of the conventional metal [44], suggesting the microstructural details of the superlattices are different from those of disordered metallic systems. This large increase in noise close to T_{MIT} could be due to the percolative transition of electrons in an inhomogeneous medium [45]. It has been predicted for such a medium from the "random void model" that noise scales as R^w, with $w = 2.1$. We find that $\frac{\delta R^2}{R^2} \propto R^w$, with $w \sim 2 \pm 0.1$, within the temperature range $140\ \mathrm{K} \leqslant T \leqslant 175\ \mathrm{K}$ for the 1ENO/1LNO SL and $200\ \mathrm{K} \leqslant T \leqslant 230\ \mathrm{K}$ for the 2ENO/1LNO SL (see the Appendix, Fig. 6). Such a classical percolation picture was reported for other oxides as well when they undergo a normal to superconducting phase transition [46,47]. It can be seen from Fig. 3 that the magnitude of noise of 1ENO/1LNO is three orders larger than that of 2ENO/1LNO. Large increases in noise have been seen in other oxide undergoing long-range charge ordering transition [38]. We speculate that because of the absence of long-range CO in the 2ENO/1LNO SL, the noise magnitude is smaller than in the 1ENO/1LNO SL.

While the origin of noise in the metallic phase can be understood from the Dutta-Horn model [48,49], such a defect-scattering-based mechanism fails to explain the peculiar behavior of noise in the temperature range $0.85 \lesssim T/T_{\mathrm{MIT}} \lesssim 1.1$. To gain better understanding of the origin of such excess noise, we investigated higher-order statistics of resistance fluctuations, which have been used to study the presence of long-range correlations undergoing magnetic, spin-glass [50], and superconducting [47] transitions. To calculate the higher-order statistics of resistance fluctuations, we computed the second spectrum. The second spectrum is a four-point correlation function of the resistance fluctuations over a chosen octave (f_l, f_h) and is defined as $S_R^{f_1}(f_2) = \int_0^\infty \langle \delta R^2(t) \rangle \langle \delta R^2(t+\tau) \rangle \cos(2\pi f_2 \tau) d\tau$, where f_1 is the center frequency of a chosen octave and f_2 is the spectral frequency. Physically, $S_R^{f_1}(f_2)$ represents the "spectral wandering" or fluctuations in the PSD with time in the chosen frequency octave [51]. To avoid artifacts in the actual signal from the Gaussian background noise, we calculated the second spectrum over the frequency octave 0.09375–0.1875 Hz, where the sample noise is significantly higher than the background noise. We plot the variation of the second spectrum $S_R^{f_1}(f_2)$ with frequency at different T for both superlattices in the Appendix (see Fig. 7). A convenient way of representing the second spectrum is through the normalized form $\sigma^{(2)}$, defined as $\sigma^{(2)} = \int_0^{f_h - f_l} S_R^{f_1}(f_2) df_2 / [\int_{f_l}^{f_h} S_R(f) df]^2$. For Gaussian fluctuations, $\sigma^{(2)} = 3$, and any deviation from this value would imply the presence of the NGC in the fluctuation spectrum [51]. As expected, $\sigma^{(2)} \sim 3$ in the metallic phase of both samples [Figs. 4(a) and 4(b)]. $\sigma^{(2)}$ starts to deviate from 3 for both samples around T_{MIT}, implying that the observation of excess noise is intimately connected to the electronic phase separation. In the case of the 1ENO/1LNO SL, $\sigma^{(2)}$ shows a peak near $T \sim T_{\mathrm{MIT}} = T_N$. On the contrary,

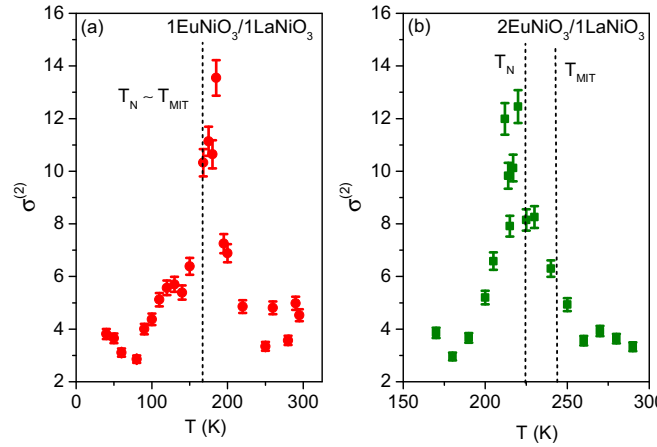

FIG. 4. (a) and (b) Plot of the normalized second spectrum $\sigma^{(2)}$ as a function of temperature for $1EuNiO_3/1LaNiO_3$ and $2EuNiO_3/1LaNiO_3$, respectively.

$\sigma^{(2)}$ reaches maximum near $T \sim T_N$ for the 2ENO/1LNO SL. This surprising observation is likely to be related to the multiband nature of these materials. The Fermi surface of the paramagnetic metallic phase consists of large hole pockets with small electron pockets [52]. As inferred from the Hall effect measurements by Ojha *et al.* [42], the metal-insulator transition results in a partially gapped Fermi surface, and the hole Fermi surface vanishes around T_N because of the nesting-driven paramagnetic to E' antiferromagnetic transition.

The length scale associated with the electronic phase separation can be estimated if we consider that the activation energy E_a corresponds to the pure elastic energy generated due to the volume difference between metallic and insulating phases [38]. The bulk moduli of $EuNiO_3$ and $LaNiO_3$ are approximately 320 and 380 GPa, respectively [53]. The out-of-plane lattice constant of the SLs shows around 0.2% expansion across the MIT [21], yielding an energy density $E_v \sim 160$–$190\ \mathrm{kJ/m^3}$ associated with the transformation. By assuming that the metallic nucleating regions are spherical with a diameter L_m, $E_a \sim 0.42$ eV corresponds to $L_m \sim 7.0$–7.4 nm. We note that a conductive-atomic force microscopy study with a spatial resolution of ~100 nm found the nucleation of metallic domains with a size of ~100–300 nm in a $NdNiO_3$ thin film [54]. Our results emphasize that nucleation of such a metallic phase happens on a much shorter length scale.

An earlier x-ray absorption spectroscopy experiment demonstrated the presence of short-range charge ordering even in the metallic phase of all $RNiO_3$ [43]. Our present noise measurements emphasize similar characteristics for both samples, such as random resistance fluctuations, $1/f$ noise for $T > T_{\mathrm{MIT}}$ and RTN in resistance fluctuations, and non-$1/f$ and non-Gaussian characterization of noise for $T > 0.85T_{\mathrm{MIT}}$. Further, the very similar length scales associated with nucleation of metallic clusters in the insulating phase in both samples also suggest that the samples have similar electronic and magnetic properties at the nanoscale. However, the much smaller noise magnitude of 2ENO/1LNO around T_{MIT} compared to the 1ENO/1LNO SL and the additional

TABLE I. Value of the Hooge parameter for different nickelates at 300 K.

System	Hooge parameter at 300 K
$1EuNiO_3/1LaNiO_3$	10^4
$2EuNiO_3/1LaNiO_3$	10^4
$LaNiO_{3-\delta}$ [55]	10^3
$SmNiO_3$ [35]	5×10^3
$NdNiO_3$ [36,37]	5×10^6

noise peak near T_N indicate that the details of the electrical transport process depend on the presence or absence of long-range charge and magnetic orderings. Complimentary microscopy experiments with subnanometer resolution should help to clarify the details of the development of long-range charge ordered phase from a short-range charge ordered phase and the magnetic nature of phase-separated phases around the transition temperatures.

IV. CONCLUSION

To summarize, we observed the presence of large excess noise around the metal-insulator and magnetic transitions in $EuNiO_3/LaNiO_3$ thin films. The appearance of RTN, causing non-$1/f$ noise below T_{MIT}, implies that the electronic phase separation is responsible for the excess noise. This is further corroborated by the observation of a large non-Gaussian noise in the insulating phase. Noise in the metallic phase shows $1/f$ behavior with the Gaussian statistics of the resistance fluctuations. Observation of the maxima of $\sigma^{(2)}$ near T_N for the 2ENO/1LNO SL is likely to be connected to the Fermi surface nesting-driven origin of E'-type antiferromagnetic ordering. Our experiments highlight the importance of studying resistance fluctuations near the phase transition which can be applied to understand the transition between two electronic phases of any system.

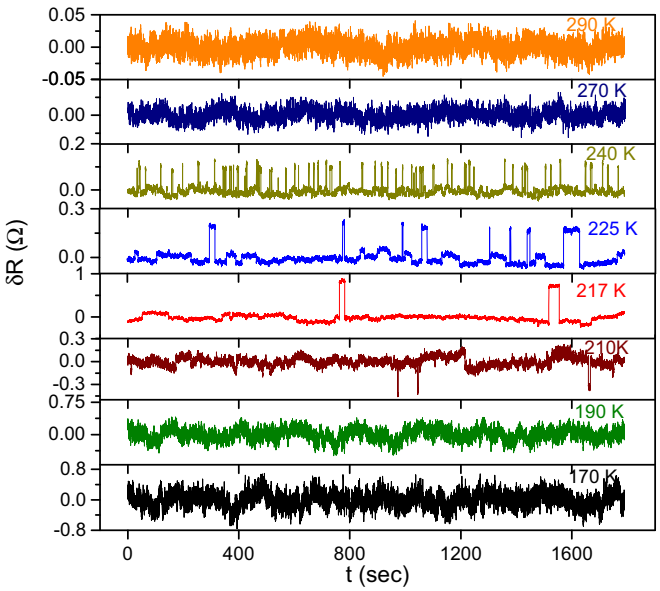

FIG. 5. Time series of resistance fluctuations at a few representative values of T for $2EuNiO_3/1LaNiO_3$.

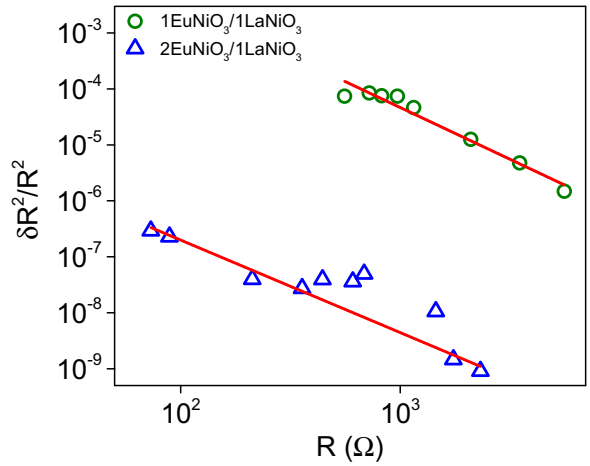

FIG. 6. Log-log plot of $\frac{\delta R^2}{R^2}$ as a function of resistance for $1EuNiO_3/1LaNiO_3$ and $2EuNiO_3/1LaNiO_3$. The red line represents the linear fit of the data to a slope of 2 ± 0.1. For details see the text.

ACKNOWLEDGMENTS

S.M. acknowledges a IISc start up grant, a DST Nanomission grant (DST/NM/NS/2018/246), and a SERB Early Career Research Award (ECR/2018/001512) for financial support. A.B. thanks SERB, DST, for financial support. J.C. is supported by the Gordon and Betty Moore Foundation EPiQS Initiative through Grant No. GBMF4534.

APPENDIX

To compare the noise level of $EuNiO_3/LaNiO_3$ with other nickelates, we calculated the Hooge parameter γ_H [56], defined as $\gamma_H = \frac{NfS_R(f)}{R^2}$ (N, total number of charge carriers,

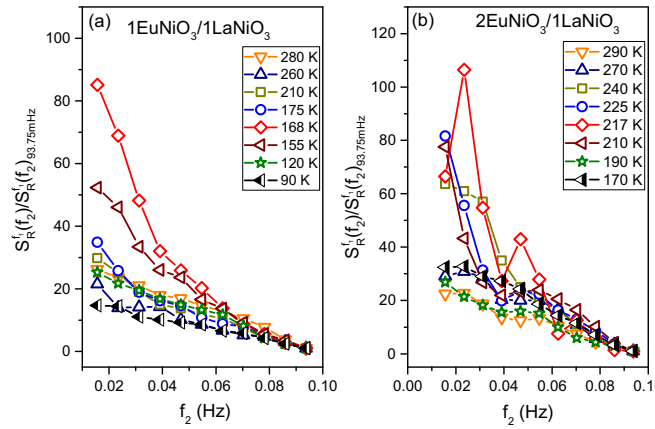

FIG. 7. (a) and (b) Plot of the second spectrum $S_R^{f_1}(f_2)$ as a function of frequency at different T for $1EuNiO_3/1LaNiO_3$ and $2EuNiO_3/1LaNiO_3$, respectively. Note that the data are scaled at 93.75 mHz to see the nature at different temperatures.

was evaluated from the Hall effect measurement). The value of γ_H for different nickelates is tabulated in Table I. The large value of γ_H suggests that the origin of the noise of these $RNiO_3$ is different from the scattering mechanism of an electron with the lattice phonon mode predicted by Hooge for metals and semiconductors [44]. A possible explanation of the large increase in noise is the classical percolation of electrons in an inhomogeneous medium [45]. Figure 5 shows the time series of resistance fluctuations of 2ENO/1LNO SL. Figure 6 gives the log-log plot of $\frac{\delta R^2}{R^2}$ as a function of resistance. Figure 7 illustrates the second spectrum $S_R^{f_1}(f_2)$ as a function of frequency.

[1] M. Imada, A. Fujimori, and Y. Tokura, Rev. Mod. Phys. **70**, 1039 (1998).
[2] Y. Tokura, Rep. Prog. Phys. **69**, 797 (2006).
[3] S. Middey, J. Chakhalian, P. Mahadevan, J. W. Freeland, A. J. Millis, and D. D. Sarma, Annu. Rev. Mater. Res. **46**, 305 (2016).
[4] S. Catalano, M. Gibert, J. Fowlie, J. Íñiguez, J.-M. Triscone, and J. Kreisel, Rep. Prog. Phys. **81**, 046501 (2018).
[5] M. L. Medarde, J. Phys.: Condens. Matter **9**, 1679 (1997).
[6] G. Catalan, Phase Transitions **81**, 729 (2008).
[7] A. Mercy, J. Bieder, J. Íñiguez, and P. Ghosez, Nat. Commun. **8**, 1677 (2017).
[8] M. K. Stewart, J. Liu, M. Kareev, J. Chakhalian, and D. N. Basov, Phys. Rev. Lett. **107**, 176401 (2011).
[9] U. Staub, G. I. Meijer, F. Fauth, R. Allenspach, J. G. Bednorz, J. Karpinski, S. M. Kazakov, L. Paolasini, and F. d'Acapito, Phys. Rev. Lett. **88**, 126402 (2002).
[10] I. I. Mazin, D. I. Khomskii, R. Lengsdorf, J. A. Alonso, W. G. Marshall, R. M. Ibberson, A. Podlesnyak, M. J. Martínez-Lope, and M. M. Abd-Elmeguid, Phys. Rev. Lett. **98**, 176406 (2007).
[11] S. R. Barman, A. Chainani, and D. D. Sarma, Phys. Rev. B **49**, 8475 (1994).
[12] T. Mizokawa, D. I. Khomskii, and G. A. Sawatzky, Phys. Rev. B **61**, 11263 (2000).
[13] H. Park, A. J. Millis, and C. A. Marianetti, Phys. Rev. Lett. **109**, 156402 (2012).
[14] S. Johnston, A. Mukherjee, I. Elfimov, M. Berciu, and G. A. Sawatzky, Phys. Rev. Lett. **112**, 106404 (2014).
[15] A. Subedi, O. E. Peil, and A. Georges, Phys. Rev. B **91**, 075128 (2015).
[16] V. Bisogni, S. Catalano, R. J. Green, M. Gibert, R. Scherwitzl, Y. Huang, V. N. Strocov, P. Zubko, S. Balandeh, J.-M. Triscone *et al.*, Nat. Commun. **7**, 13017 (2016).
[17] J. Shamblin, M. Heres, H. Zhou, J. Sangoro, M. Lang, J. Neuefeind, J. A. Alonso, and S. Johnston, Nat. Commun. **9**, 86 (2018).
[18] S. B. Lee, R. Chen, and L. Balents, Phys. Rev. Lett. **106**, 016405 (2011).
[19] S. B. Lee, R. Chen, and L. Balents, Phys. Rev. B **84**, 165119 (2011).
[20] M. Hepting, M. Minola, A. Frano, G. Cristiani, G. Logvenov, E. Schierle, M. Wu, M. Bluschke, E. Weschke, H.-U. Habermeier, E. Benckiser, M. Le Tacon, and B. Keimer, Phys. Rev. Lett. **113**, 227206 (2014).
[21] S. Middey, D. Meyers, M. Kareev, Y. Cao, X. Liu, P. Shafer, J. W. Freeland, J.-W. Kim, P. J. Ryan, and J. Chakhalian, Phys. Rev. Lett. **120**, 156801 (2018).
[22] R. Scherwitzl, P. Zubko, I. Gutierrez Lezama, S. Ono, A. F. Morpurgo, G. Catalan, and J.-M. Triscone, Adv. Mater. **22**, 5517 (2010).
[23] J. Shi, S. D. Ha, Y. Zhou, F. Schoofs, and S. Ramanathan, Nat. Commun. **4**, 2676 (2013).
[24] J. Shi, Y. Zhou, and S. Ramanathan, Nat. Commun. **5**, 4860 (2014).
[25] S. D. Ha, J. Shi, Y. Meroz, L. Mahadevan, and S. Ramanathan, Phys. Rev. Appl. **2**, 064003 (2014).
[26] B. K. Jones, IEE Proc.-Circuits, Devices Syst. **149**, 13 (2002).
[27] R. Koushik, M. Baenninger, V. Narayan, S. Mukerjee, M. Pepper, I. Farrer, D. A. Ritchie, and A. Ghosh, Phys. Rev. B **83**, 085302 (2011).
[28] U. Chandni, A. Ghosh, H. S. Vijaya, and S. Mohan, Phys. Rev. Lett. **102**, 025701 (2009).
[29] H. K. Kundu, S. Ray, K. Dolui, V. Bagwe, P. R. Choudhury, S. B. Krupanidhi, T. Das, P. Raychaudhuri, and A. Bid, Phys. Rev. Lett. **119**, 226802 (2017).
[30] J. Clarke and T. Y. Hsiang, Phys. Rev. B **13**, 4790 (1976).
[31] D. Babić, J. Bentner, C. Sürgers, and C. Strunk, Phys. Rev. B **76**, 134515 (2007).
[32] F. Reif, *Fundamentals of Statistical and Thermal Physics* (Waveland, Long Grove, IL, 2009).
[33] M. B. Weissman, Rev. Mod. Phys. **60**, 537 (1988).
[34] A. Ghosh, S. Kar, A. Bid, and A. Raychaudhuri, arXiv:cond-mat/0402130.
[35] A. Sahoo, S. D. Ha, S. Ramanathan, and A. Ghosh, Phys. Rev. B **90**, 085116 (2014).
[36] A. M. Alsaqqa, S. Singh, S. Middey, M. Kareev, J. Chakhalian, and G. Sambandamurthy, Phys. Rev. B **95**, 125132 (2017).
[37] R. S. Bisht, S. Samanta, and A. K. Raychaudhuri, Phys. Rev. B **95**, 115147 (2017).
[38] A. Bid, A. Guha, and A. K. Raychaudhuri, Phys. Rev. B **67**, 174415 (2003).
[39] S. Middey, D. Meyers, S. K. Ojha, M. Kareev, X. Liu, Y. Cao, J. W. Freeland, and J. Chakhalian, Phys. Rev. B **98**, 045115 (2018).
[40] S. Middey, D. Meyers, R. K. Patel, X. Liu, M. Kareev, P. Shafer, J.-W. Kim, P. J. Ryan, and J. Chakhalian, Appl. Phys. Lett. **113**, 081602 (2018).
[41] J.-S. Zhou, J. B. Goodenough, and B. Dabrowski, Phys. Rev. Lett. **94**, 226602 (2005).
[42] S. K. Ojha, S. Ray, T. Das, S. Middey, S. Sarkar, P. Mahadevan, Z. Wang, Y. Zhu, X. Liu, M. Kareev, and J. Chakhalian, Phys. Rev. B **99**, 235153 (2019).
[43] C. Piamonteze, H. C. N. Tolentino, A. Y. Ramos, N. E. Massa, J. A. Alonso, M. J. Martínez-Lope, and M. T. Casais, Phys. Rev. B **71**, 012104 (2005).
[44] F. N. Hooge, Physica **60**, 130 (1972).
[45] A.-M. S. Tremblay, S. Feng, and P. Breton, Phys. Rev. B **33**, 2077 (1986).

[46] L. B. Kiss and P. Svedlindh, IEEE Trans. Electron Devices **41**, 2112 (1994).
[47] G. N. Daptary, S. Kumar, P. Kumar, A. Dogra, N. Mohanta, A. Taraphder, and A. Bid, Phys. Rev. B **94**, 085104 (2016).
[48] P. Dutta and P. Horn, Rev. Mod. Phys. **53**, 497 (1981).
[49] G. N. Daptary, C. Sow, S. Sarkar, S. Chiniwar, P. A. Kumar, A. Sil, and A. Bid, Phys. B (Amsterdam, Neth.) **511**, 74 (2017).
[50] G. N. Daptary, C. Sow, P. S. A. Kumar, and A. Bid, Phys. Rev. B **90**, 115153 (2014).
[51] G. T. Seidler and S. A. Solin, Phys. Rev. B **53**, 9753 (1996).
[52] R. Eguchi, A. Chainani, M. Taguchi, M. Matsunami, Y. Ishida, K. Horiba, Y. Senba, H. Ohashi, and S. Shin, Phys. Rev. B **79**, 115122 (2009).
[53] J.-S. Zhou, J. B. Goodenough, and B. Dabrowski, Phys. Rev. B **70**, 081102(R) (2004).
[54] D. Preziosi, L. Lopez-Mir, X. Li, T. Cornelissen, J. H. Lee, F. Trier, K. Bouzehouane, S. Valencia, A. Gloter, A. Barthélémy *et al.*, Nano Lett. **18**, 2226 (2018).
[55] A. Ghosh, A. K. Raychaudhuri, R. Sreekala, M. Rajeswari, and T. Venkatesan, J. Phys. D **30**, L75 (1997).
[56] F. N. Hooge, Phys. Lett. **29**, 139 (1969).